CHAPTER 5

Multiscaling Analysis in Distributed Modeling and Remote Sensing: An Application Using Soil Moisture

Ralph Dubayah, Eric F. Wood, and Daniel Lavallée

INTRODUCTION

One of the major uses of geographical information systems (GIS) is to provide an environment that facilitates distributed modeling. Such modeling frequently requires the integration of diverse input data such as point ground measurements, thematic maps, and areal remotely-sensed observations. The required input fields rarely are available at the desired modeling scale and their use at a scale other than that at which they were observed (e.g., via resampling) is not always straightforward. Conversely, if the data are allowed to determine the scale at which the modeling is to take place, the resulting model outputs may not be suitable for addressing the research problem in question. In general, modelers tend to find some middle ground and make decisions on modeling scale based on the resolution of the available input data, computational resources, and their perception of the required resolution of the outputs. However, these decisions are not without consequences, the most important of which is that model outputs may vary as a function of scale.

The recognition of such scale effects has led to research into the scaling properties of environmental fields. The term "scaling" has come to have multiple definitions, depending not only on the general discipline (e.g., geography, physics, or ecology) but the application within the discipline (e.g., within geography, remote sensing as opposed to cartography). This has led to some confusion about the term. In general, a process is said to be scaling if no characteristic length scale exists, i.e., the statistical spatial properties of the field do not exhibit scale-dependent behavior.

Why do scaling problems occur; that is, why cannot data or model outputs simply be scaled up or down to meet the task at hand? Part of the answer is that remotely

1-56670-104-X/97/$0.00+$.50

sensed and gridded model output fields share an important property concerning their spatial variability: both are inherently scale-limited. For remotely sensed observations, little information can be inferred below the resolution of the sensor. For distributed outputs, the model grid spacing determines the smallest spatial scale at which fields may be realized. The limitations imposed by resolution and grid spacing, or their interaction, can hamper modeling efforts over large areas, especially when the processes are spatially autocorrelated. Such processes often scale non-linearly such that the moments of the field (e.g., the mean and the variance) obtained at one spatial scale may be significantly different from those obtained at a larger or smaller scale.

An important environmental variable whose scaling properties have generated considerable interest is soil moisture. Soil moisture is highly variable over a large range of scales, often showing as much variability over a distance of meters as it does over hundreds of kilometers. This behavior is typical of scaling fields. Its spatial scaling properties are poorly understood because it is so difficult to model and measure. This in turn confounds validation efforts given the problematic comparison of sparse, point ground measurements with areal outputs usually produced by distributed models. Passive and active microwave remote sensing techniques have been developed that provide soil moisture estimates in the first 5 cm or so of the soil column for predominantly bare or sparsely vegetated surfaces. These remote methods may provide improved validation and modeling capability, but the effects of resolution (scale) on retrieved measurements are largely unknown.

Some of the major scaling issues involved with modeling in general, and soil moisture in particular, may be better understood with the following example. Consider a hydrological model with distributed input layers such as radiation, precipitation, temperature, topography and soils at 1 km resolution. If the required resolution of an output soil moisture field is to be 10 km, two choices are available: (a) aggregate the input layers first to 10 km, to produce 10 km output fields; or, (b) keep the input fields at 1 km resolution, run these through the model to produce 1 km output fields, and then aggregate the outputs to 10 km grid spacing. Either method is legitimate; however, the results from each may not be the same. The degree to which they differ depends in part on the non-linearity of the model equations relative to the input fields, the spatial autocorrelation and scaling properties of those fields, and the amount of model spatial interaction. Modeling at a fine scale and aggregating at output ensures that no fine scale variability is lost, but this option is often not available, either because of lack of data or the increased computational burden. Efforts to parameterize sub-grid scale variability are a means for adjusting the statistical properties of fields to incorporate unmodeled fine scale variability (such parameterizations are used frequently in the climatological and hydrological sciences, where non-linearity is common).

This modeling problem may be complicated further by scaling effects in remote sensing data frequently used to derive input fields or validate outputs. The transformation of sensor radiances to environmental fields may itself be non-linear. For example, surface thermal radiance is non-linearly related to surface temperature through the Planck equation. Similarly, microwave radiance is non-linearly related

to brightness temperature, which is then related to near-surface soil moisture state. This leads to another type of scaling problem where the areal average of temperatures at a fine resolution may not be equal to the temperature derived from averaging the radiances first for the same area. Thus, there is a dependence of temperature on scale, which may then be convolved with the first situation of non-linear model equations (if the fields are used to drive a model).

These aspects of scaling have been recognized for some time, although there has been little in the way of a framework for exploring them. The common mode of exploration has been to realize fields at fine scales, aggregate, and compare the results with those realized at coarse scales (e.g., see Wood and Lakshmi, 1993; Sellers et al., 1995). The hope is that either linear or otherwise known relationships may be found that link field statistics, at least for some limited range of scales. Otherwise, if the fields do not scale linearly, or if we do not know how to model the non-linearity, we are forced to model at the scale of interest, regardless of its practicality.

Development of a strategy for scaling in distributed modeling is a formidable task, as it involves the complex interactions among data and model transforms just described. However, a framework for the systematic exploration of scaling recently has been developed. It has been shown that non-linear spatial variability among scales may be a consequence of fields that are generated by what are known as cascade processes (e.g., see among others, Monin and Yaglom, 1987; Gupta and Waymire, 1990). In such processes, the field flux (e.g., of moisture, energy, etc.) is the result of some cascading down of large scale (large area) fluxes to successively smaller and smaller scales. Cascade processes can produce fields which exhibit "multiscaling" or "multifractal" behavior, characterized by spatial or temporal scaling exponents which are non-linear with respect to the order of statistical moment (e.g., see Schertzer and Lovejoy, 1987; Meneveau and Sreenivasan, 1987; and Marshak et al., 1994). The development of a theoretical basis, and accompanying data analysis methods (e.g., see Davis et al., 1994), suggests new approaches for the systematic analysis of the multiscale variability of environmental fields, approaches that seem particularly well suited to the issue of scaling within GIS. It is this multiscaling perspective that directs the focus of our research.

In this chapter we explore the multiscaling properties of soil moisture fields for a small basin in Oklahoma, the Little Washita, derived in two ways: (1) from a passive microwave sensor at 200-m resolution; and, (2) output from a distributed energy and water balance model at 30-m grid spacing. Obtained during the Washita '92 field experiment (Jackson and LaVine, 1994), these data sets provide a unique opportunity to develop a better understanding of how remotely sensed and modeled fields may be integrated to address scaling issues. The remainder of this chapter is organized as follows. We briefly present some basic concepts concerning simple scaling and multiscaling, including equations relating moments at differing scales. The data sources for the derived soil moisture fields are then described. We next present the methodology and results of a multiscale analysis of the fields for nine successive days during a period of soil moisture dry down. Our analysis is based on empirical plots of log–log relationships of statistical moment as a function of

scale. From these plots we determine scaling exponents and look for signals of multiscaling. Lastly, we discuss a relevant application, prediction of the statistical behavior of fields at scales other than the observational scale, and present some caveats about the use of multiscale analysis as well as its possibilities.

SCALING AND MULTISCALING PROPERTIES

It recently has been suggested that many geophysical processes may exhibit multiscale or multifractal behavior (among others, spatial rainfall: Gupta and Waymire, 1990, 1993; turbulence: Schmitt et al., 1992; microwave brightness temperatures: Jourdan et al., 1993; topography: Lavallée et al., 1993; Weissel et al., 1994; river basins: Rodriguez-Iturbe et al., 1994; and clouds: Tessier et al., 1993). A multiscaling framework allows for spatially heterogeneous processes to operate and produce spatially heterogeneous fields characterized by scaling exponents that are non-linear with respect to the order of statistical moment. Soil moisture fields are the result of many different processes acting over different scales, such as topography, soil characteristics, precipitation, vegetation distribution, and so on. As a result, a multiscaling framework seems an appropriate place from which to examine the scaling properties of these fields.

Simple Scaling and Multiscaling

For remote sensing or raster GIS, fields are taken over a grid with a particular grid spacing and extent. If we average all the grid cells within the image or grid, we will have one value at the coarsest grid spacing or scale factor, denoted by $\lambda = 1$. As resolution is increased, from this single value, to 4, 16, 64 values, and so on, down to the finest resolution, we have scale factors which decrease as $\lambda = 1/1, 1/2, 1/4, 1/8$, averaging over squares of decreasing size whose sides have length λ. A process λ is defined as spatially scaling if the following is true:

$$E[\phi_\lambda] \propto \lambda^K E[\phi_1] \tag{1}$$

where the notation $E[\phi_\lambda]$ denotes the expected value (or statistical ensemble average) of the field at scale factor λ. This expectation is equal to the expected value of the field at the scale factor $\lambda = 1$, times a scaling function λ^K, where K is the scaling exponent. Note two points. First, $\lambda = 1$ need not refer to the actual coarsest aggregation possible for a field of a given extent, but is simply a reference point. For example, $\lambda = 1$ could correspond to an aggregation of 64×64 grid cells in a field of size 512×512, and thus $\lambda = 1/2$ would refer to an aggregation of 32×32, and so on. Secondly, $\lambda \leq 1$ because it is defined as the ratio of a given resolution to that of the coarsest resolution, i.e., the reference resolution or the largest scale factor, following the convention of Gupta and Waymire (1990). Often the scale factor is defined in an opposite sense, as λ^{-1} (e.g., as in Schertzer and Lovejoy, 1987), where the largest scale factor corresponds to the finest resolution. In this case, the scaling

exponents, though of identical magnitude, are positive, whereas with the definition used here, they are negative.

Eq. 1 may be generalized to the expected moments of a field other than the mean (first moment) as:

$$E[(\phi_\lambda)^q] \propto \lambda^{K(q)} E[(\phi_1)^q] \tag{2}$$

where q is the order moment and where there are now a set of scaling exponents, $K(q)$ associated with the moments.

A process is said to be simple scaling if the $K(q)$ are linearly related to the order of moment q such that:

$$E[(\phi_\lambda)^q] \propto \lambda^{qC} E[(\phi_1)^q] \tag{3}$$

For simple scaling there is only one scaling exponent C and the process is said to be "fractal" or "monofractal." The expected moments of a field can then be related to this single value as a function of scale. For multiscaling the $K(q)$ are non-linearly related to q, with a set of scaling exponents $K(q)$ exactly as given in Eq. 2 above, i.e., the exponents are not linear with respect to q. The curve of $K(q)$ for a multiscaling field is typically convex (downwards, with our definition of λ, i.e., negative second derivatives of $K(q)$ with respect to q), and this behavior now has become the distinguishing empirical feature of multiscaling (Gupta and Waymire, 1990; Meneveau and Sreenivasan, 1991; Rodriguez-Iturbe et al., 1994; Weissel et al., 1994). (Note that the non-linear behavior of $K(q)$ may be best observed for small values of q, usually with $0 < q < 1$).

Eq. 2 has an important consequence for scaling applications in remote sensing and GIS. By definition, the scaling exponents are not a function of scale (although empirically we may observe them only over a limited range of scales). If the $K(q)$ are known, or if we have determined *a priori* that they can be found accurately at the scale of observation, this implies a process may be observed or modeled at one scale, and its statistical properties inferred at another scale. Given a remotely sensed field with a given scale factor λ whose moments are calculated, the moments at another scale factor λ_2 can be found using Eq. 2.

DATA SOURCES

The data for this work are derived from the Washita '92 field experiment in Oklahoma during June 1992 (Jackson and LaVine, 1994). The Little Washita River basin is a 525-sq. km watershed which has a mixture of pasture and agricultural land use. Remotely sensed data were acquired from aircraft June 10 to 18 (except June 15). An energy and water balance model also was run for this same period to estimate near surface soil moisture state. During the nine days, there was a consistent dry down of near surface soil moisture.

ESTAR

ESTAR refers to the electronically scanned thinned array radiometer airborne remote sensing instrument, which measures the microwave emission from the surface at 1.4 GHz (L-Band). At this wavelength, the intensity of the observed radiation is proportional to the brightness temperature (which is the product of the surface emissivity and the soil thermodynamic temperature.) Also at this wavelength, the soil emissivity is particularly sensitive to volumetric soil moisture (Wang and Schmugge, 1980; Dobson et al., 1985). Using a soil moisture retrieval algorithm that incorporates information about soil texture and surface cover, brightness temperatures are converted into estimates of soil moisture.

During the past 15 years, there has been a steady progression of field experiments that have demonstrated the success of using passive microwave remote sensing for the determination of soil moisture. Reviews are available in Jackson and Schmugge (1986) and Engman (1991). L-band passive microwave remote sensing for soil moisture can make corrections for vegetation up to canopies approximately the size of mature corn fields (Jackson and Schmugge, 1991) which makes this technique useful for many applications.

The ESTAR instrument is the most current version of airborne microwave radiometers developed by NASA and flown on NASA's C-130 and P3 aircraft. The instrument has a resolution of ±8° and a swath width of ±45°. When imaging at 7000 ft, this results in post-processing resolution of approximately 200 m. It has been applied to measure regional soil moisture over the Walnut Gulch, AZ watershed (Jackson et al., 1993), a semi-arid environment, and the Little Washita, OK watershed. It is this latter soil moisture product that we have used in the analysis presented in this chapter.

Soil Moisture Modeling

Soil moisture was modeled using a distributed water and energy balance model at 30 m grid spacing, and includes vegetation canopy effects of interception, surface storage, and transpiration based on Penman-Monteith. The soil column uses a three-layer representation which includes a thin upper layer, a root zone/transmission layer and a lower saturated layer. Surface infiltration is modeled using Philip's equation and the soil evaporation through a resistance formulation. Topographic effects on the lateral, downslope transmission of water in the saturated zone are modeled using the concepts of TOPMODEL (Beven and Kirkby, 1979). Famiglietti and Wood (1994a) describe the model and Famiglietti and Wood (1994b) its application to the Kings Creek, KS watershed which was part of the First ISLSCP Field Experiment (FIFE) (Sellers et al., 1988). Extensions to the model include the thin upper layer and the resistance parameterization to the soil evaporation.

The model is usually run either in the full energy balance mode in which incoming solar radiation, downwelling long wave radiation and precipitation are the forcing variables; or in a Penman-Monteith parameterization which utilizes net surface radiation. Surface meteorological data (wind, air temperature, and humidity) are also required to drive the model.

Model parameters can be divided up into topographic parameters, soil parameters, and vegetation parameters. The topographic parameter is the soil–topographic index, $\ln(\alpha T_e/T_i \tan\beta)$, where for location i (a unit length of contour) within a watershed, α represents the upslope contributing area whose flow paths cross i, T_i is the local soil transmissivity, β is the local slope, and T_e is the watershed average soil transmissivity. This index is estimated using digital elevation and soil data. Soil parameters can be estimated from soil texture data using a variety of empirical relations (for example see Rawls et al., 1982). Vegetation parameters represent the biophysical controls on evapotranspiration and the interaction of the canopy with the atmosphere.

In the model runs described here, the upper thin soil layer was 10 cm in depth. The model was run for 9 days (June 10 to 18, 1992) at a 3-h time step using meteorological data collected during the experiment.

MULTISCALING ANALYSIS

We estimated the scaling exponents of each of the ESTAR and model soil moisture fields as follows. First, a basin mask was applied to each image to limit our analyses to soil moisture values within the watershed. Only the northern half of the watershed was imaged by ESTAR (see Figure 1). Next, realizations of each field at different scale factors were found by aggregating pixel values. The largest scale factor, corresponding to the coarsest scale ($\lambda = 1$), used aggregations of 8×8 pixels for the ESTAR data. The reason for such a limited aggregation size was that each image contained quite a few missing data values, for example over roads or heavy vegetation. These missing data were excluded from the computation of the moments at each level of aggregation. If a particular pixel at the smallest scale factor had a missing value, all subsequent aggregations involving that pixel were also treated as missing. The largest aggregation size that also included a reasonable number of pixels from which to calculate the moments was then 8×8 (1600 m). For the model fields, the largest scale factor had an aggregation size of 128×128 pixels (3840 m) with smallest scale factor equal to 1/128 (30 m).

The second through sixth moments were then calculated for each image at each scale factor and the value of the moment plotted against scale factor in logarithmic space. The first moment was excluded because the mean of an image should not change as pixels are aggregated except for a variable support size with scale, as discussed below. Refering to Eq. 2, the slopes of these log–log lines of moment vs. scale were then calculated to estimate $K(q)$ using unweighted least-squares regression. Finally, the $K(q)$ were plotted as a function of q to look for signals of multiscaling. Before we present the results of the scaling analysis, we first compare model mean and standard deviation with those obtained from ESTAR.

The mean soil moisture for modeled and remotely sensed fields agreed well, an encouraging result (see Tables 1 and 2, and Figure 1). Because the southern portion of the basin was not imaged by ESTAR, only that portion of the modeled fields that overlaps the ESTAR imagery was used to find the mean and standard deviation (but the higher order moments were calculated using the full basin, as shown in

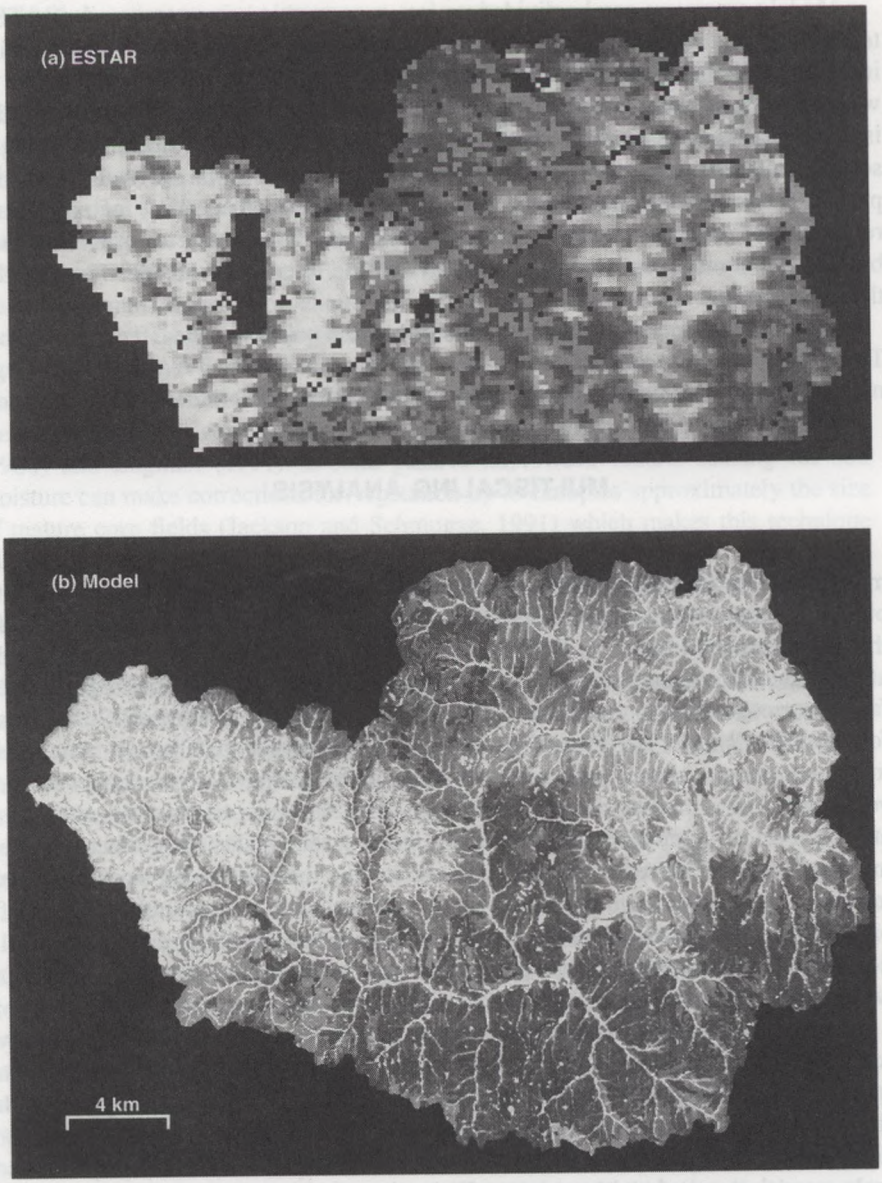

Figure 1 ESTAR (a) and water and energy balance model (b) soil moisture fields for June 10, 1992. The resolution of the ESTAR imagery is 200 m, and the grid spacing of the model fields is 30 m. The black areas in the ESTAR imagery are missing data (the diagonal line running south to north is a road). Each image has been histogram-equalized separately to highlight the spatial variability present, so direct comparisons among grey levels are misleading. Basin statistics are given in Tables 1 and 2.

Figure 1). The standard deviations were quite different between the two sources. The standard deviation of the modeled fields at 30-m grid spacing increased with

Table 1 Mean, Standard Deviation and Scaling Exponents for the Energy and Water Balance Model Soil Moisture Fields (30-m Resolution)

Date	Mean [%]	σ[%]	$K(2)$	$K(3)$	$K(4)$	$K(5)$	$K(6)$
June 10	25.723	14.095	−0.039	−0.100	−0.170	−0.245	−0.322
June 11	23.288	14.655	−0.053	−0.134	−0.226	−0.321	−0.419
June 12	21.289	15.067	−0.067	−0.170	−0.284	−0.400	−0.516
June 13	19.662	15.384	−0.083	−0.207	−0.341	−0.476	−0.609
June 14	17.888	15.701	−0.103	−0.255	−0.416	−0.574	−0.728
June 15	16.591	15.955	−0.122	−0.297	−0.478	−0.654	−0.825
June 16	15.800	16.125	−0.135	−0.324	−0.518	−0.706	−0.886
June 17	14.892	16.185	−0.149	−0.356	−0.566	−0.767	−0.960
June 18	14.358	16.213	−0.158	−0.376	−0.594	−0.804	−1.004

Note: Mean and standard deviation are found only for the areas of the basin that overlap with the ESTAR imagery. The scaling exponents are calculated from the entire Little Washita basin.

Table 2 Mean, Standard Deviation and Scaling Exponents for the ESTAR Soil Moisture Fields (200-m Resolution)

Date	Mean [%]	σ[%]	$K(2)$	$K(3)$	$K(4)$	$K(5)$	$K(6)$
June 10	22.576	6.586	−0.079	−0.153	−0.247	−0.360	−0.492
June 11	20.411	6.031	−0.084	−0.157	−0.248	−0.356	−0.480
June 12	19.928	5.824	−0.086	−0.157	−0.242	−0.341	−0.454
June 13	17.914	5.691	−0.093	−0.169	−0.257	−0.356	−0.466
June 14	19.558	5.949	−0.094	−0.159	−0.238	−0.331	−0.438
June 16	16.986	5.184	−0.099	−0.178	−0.270	−0.377	−0.499
June 17	15.011	5.058	−0.094	−0.173	−0.266	−0.372	−0.489
June 18	11.591	5.191	−0.127	−0.226	−0.336	−0.455	−0.586

dry down (however, the second moment of the model data decreased at this same spacing). We would not expect the standard deviation of a field at 30 m to match that at 200 m, so we aggregated the model results to 200 m and recalculated the standard deviation. The model standard deviation, though still significantly higher than that of the ESTAR data, did however now decrease with dry down.

ESTAR Fields

Figure 2 shows plots of moment vs. scale factor for all days. There is excellent log–log linearity in all cases. The scaling exponents $K(q)$ were found by determining the slope of each of these lines, the results of which are summarized in Table 2. Although the r^2 values were always greater than 0.98, and generally greater than 0.99, the range of scale factors over which the $K(q)$ are estimated is narrow (from 200 to 1600 m).

Plots of $K(q)$ as a function of q are shown in Figure 3. For all days these curves show signals of multiscaling, namely non-linear growth in $K(q)$ with order moment, and convex shape. The scaling exponents for a particular moment clearly differ with day, but there is no unambiguous change related to mean soil moisture conditions during the dry down. However, the last three days, June 16 to 18, and in particular,

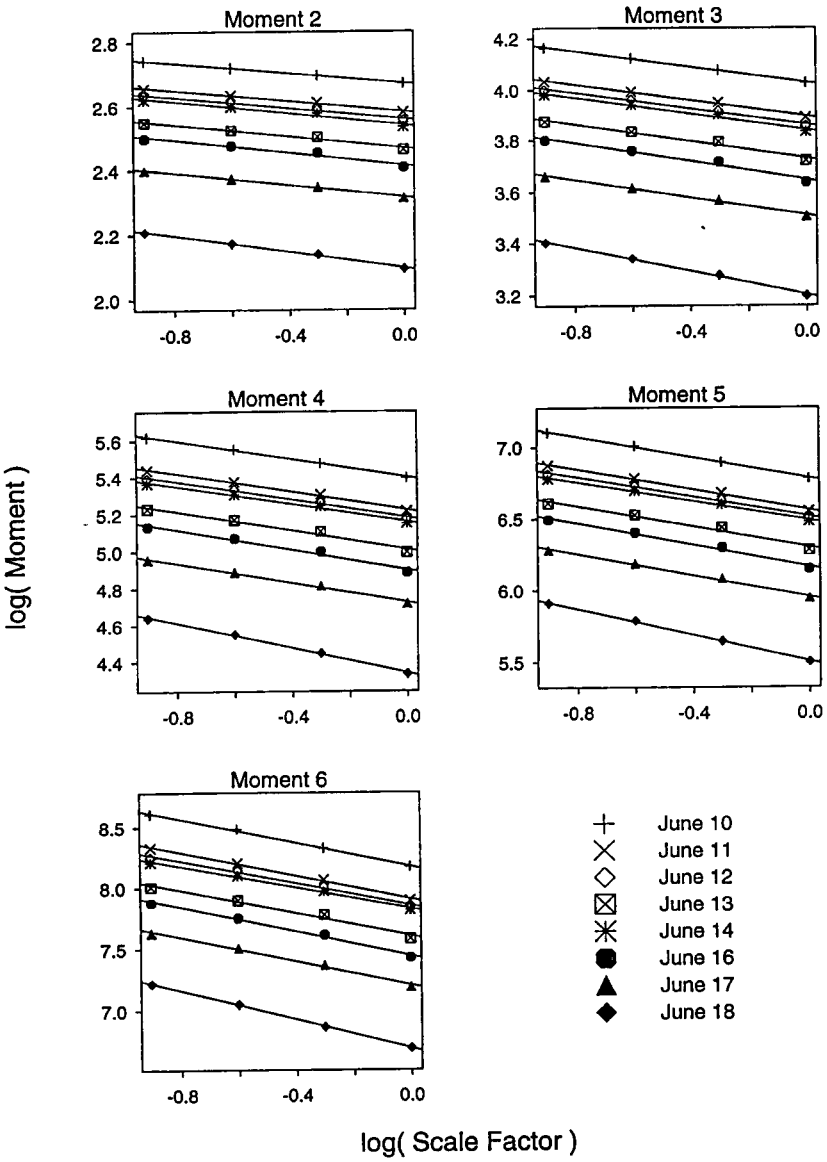

Figure 2 Plots of log(moment) vs. log(scale factor) for the ESTAR imagery. The slopes of these lines estimate $K(q)$. The range of scale factors uses aggregations over areas from 200 to 1600 m.

June 18, do have the smallest $K(q)$ values, and thus, will have smaller moments for a given scale factor. The second scaling exponent $K(2)$ does show a definite decrease with day for all days except one.

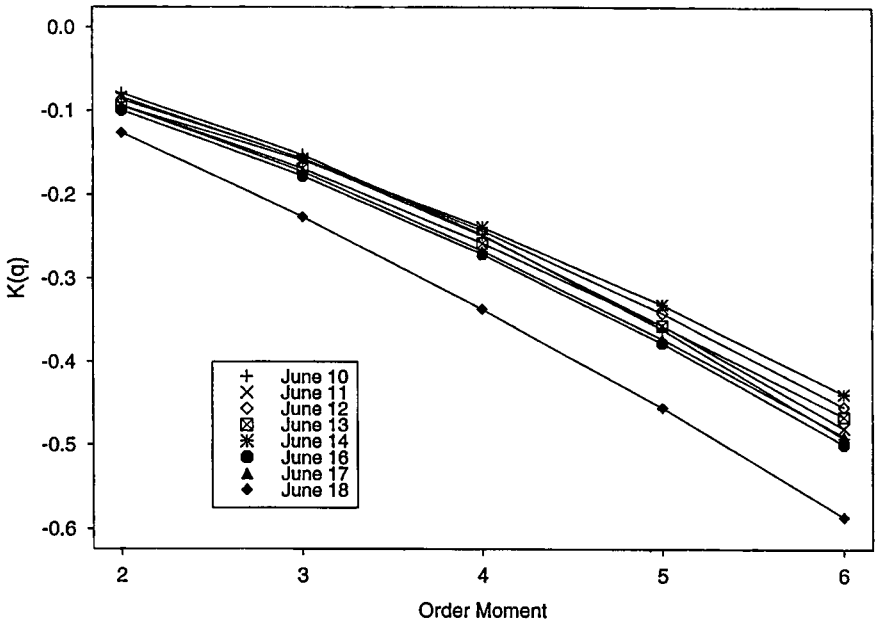

Figure 3 Plots of the curves $K(q)$ as a function of the order moment (q) for the ESTAR imagery. The curves show the signals of multiscaling: non-linear growth of the $K(q)$ and convex shape.

Modeled Fields

The modeled fields also show reasonable log–log linearity over a wide range of scales; however, the curves are slightly concave for some days and moments (Figure 4). Slightly different $K(q)$ values would be estimated depending on the range of scale factors used (we used the entire range). Table 1 lists the scaling exponents found from Figure 4. In contrast to the ESTAR fields, all moments monotonically decrease with dry down. This is seen in Figure 5 showing $K(q)$ as a function of q. There are signals of multiscaling for days June 10 to 13, where the curves are non-linear and convex. On and following June 14, the curves are either straight or slightly concave. The behavior of these curves requires further study.

DISCUSSION

As given in Tables 1 and 2, the $K(q)$ can be quite different between the ESTAR and model fields. This is seen more clearly in Figure 6. Restricting our comparison to those days when the model fields showed signals of multiscaling, the $K(q)$ are always larger (less negative) for the model fields except on June 13. The degree of similarity or dissimilarity of the spatial scaling properties of each field, however, is difficult to determine based on the $K(q)$ alone. We show below how this information can be used in a more applied fashion.

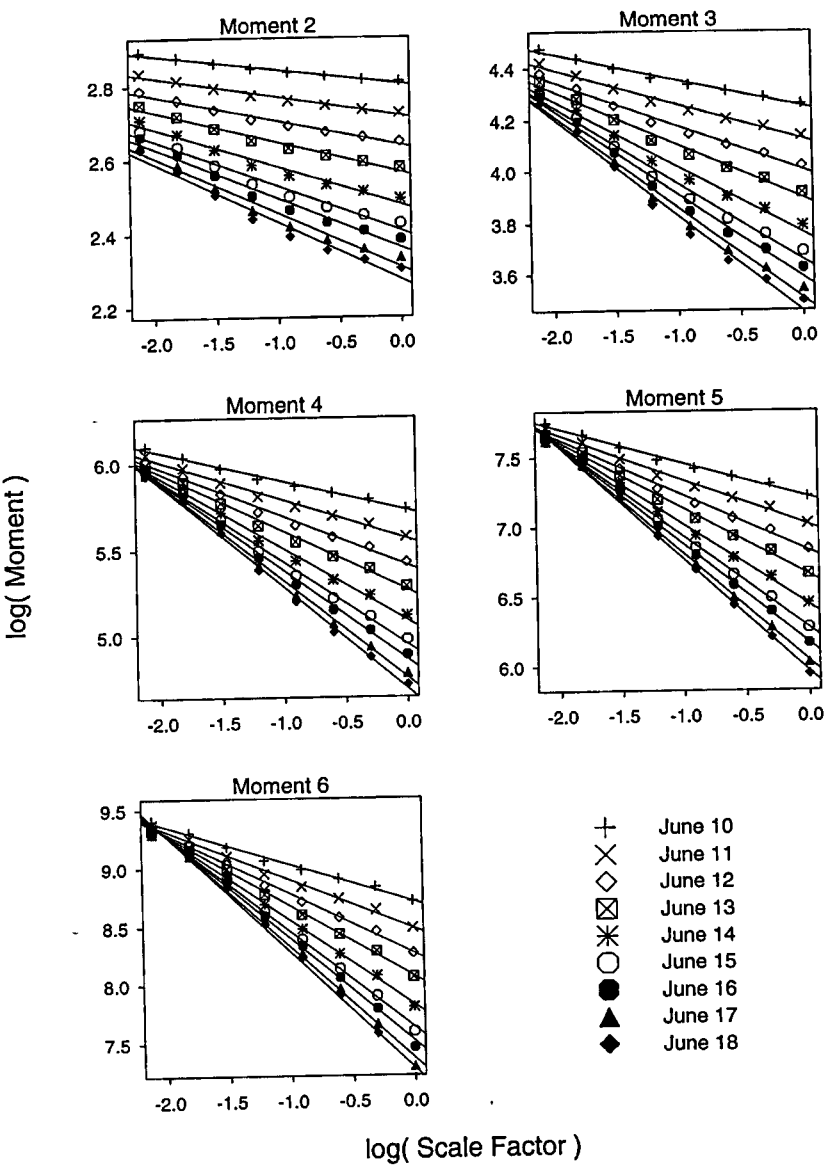

Figure 4 As in Figure 2, plots of log(moment) vs. log(scale factor) for the water and energy balance soil moisture fields. The range of scale factors uses aggregations over areas from 30 to 3840 m. Note the slight non-linearity in some of the plots.

Prediction at Other Scales

As discussed earlier, Eq. 2 allows for the inference of the statistical properties of a field at scales other than those modeled. As an example, consider the ESTAR and the modeled soil moisture fields for June 10 and their second moment. As the

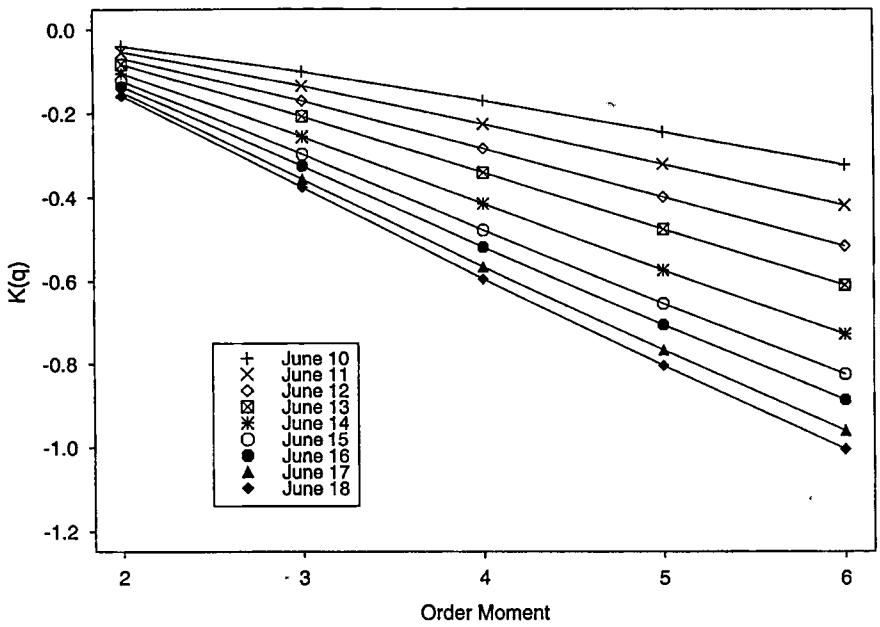

Figure 5 As in Figure 3, plots of the curves $K(q)$ as a function of the order moment (q) for the modeled fields.

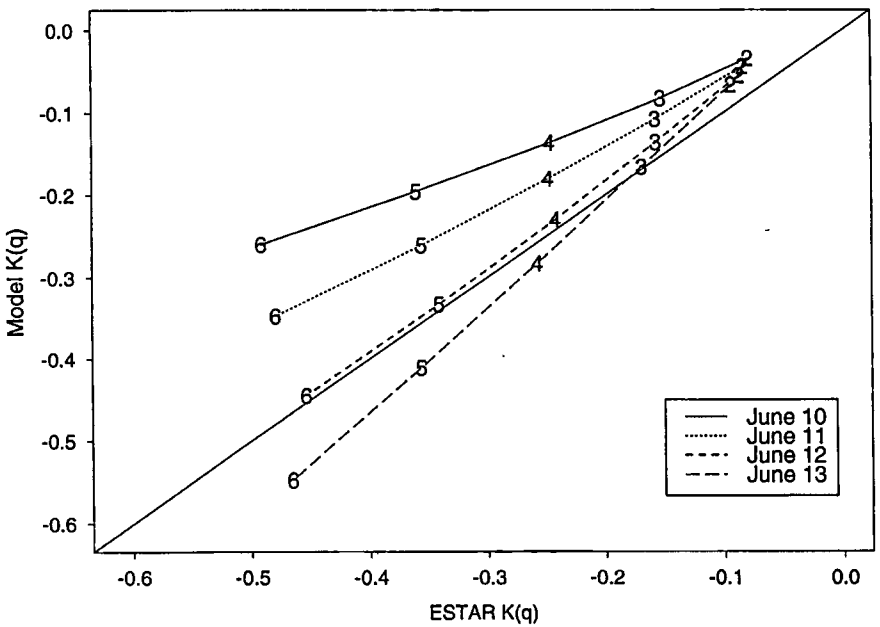

Figure 6 Model scaling exponents vs. ESTAR exponents for the four days when both showed signals of multiscaling. Each line is a day and the numbers within a line are the order moment. The 1:1 line runs diagonally.

scaling exponents are determined from the slopes of the moments vs. scale factor, the degree of linearity in these plots determines the stability of the estimates of $K(q)$ at various scales. In Figures 2 and 4, the curves are fairly linear over all scales so we should be able to accurately estimate the scaling exponents from only a few points, say at the three largest scale factors. Estimating $K(q)$ in this way is equivalent to estimating the exponents only having realizations of the field at those scales. For the modeled fields, it is the equivalent of aggregating grid cells to that scale (but the outputs may *not* be the same as aggregating input variable layers and running the model at the coarser grid spacing).

Suppose, based on *a priori* studies, that we have found that scaling of both fields is usually well behaved, i.e., that we see linear behavior over the range of scales (as in Figures 2 and 4). Further, suppose we have available only 800-m remotely sensed fields and only model fields at 960-m grid spacing. If we aggregate the ESTAR soil moisture field to simulate the 800-m data set, we obtain $K(2) = -0.089$, with a second moment value of 499, using only the 800- and 1600-m aggregations (the value of the second moment is that obtained at 800 m). Similarly, if we aggregate the model field to 960 m, we find $K(2) = -0.026$, with a second moment value of 670, again using only this realization and the next two aggregations up (1920 and 3840 m). We then predict the second moment for the ESTAR field at 200 m using Eq. 2 (ignoring any small additive constants of proportionality):

$$E[(\phi_\lambda)^2] \approx [1/4]^{-0.089} \times 499 = 564$$

where the scale factor $\lambda = 1/4$ is the ratio of the pixel lengths (200/800). The predicted second moment for the model soil moisture field at 30 m is:

$$E[(\phi_\lambda)^2] \approx [1/32]^{-0.026} \times 670 = 733$$

where the scale factor $\lambda = 1/32$ is the ratio of the pixel lengths (30/960). These compare reasonably well to the actual values of 553 and 778, respectively. Thus, we have attempted to predict variability below the actual modeling scales.

As another example, we may attempt to predict the model variability at 30 m using the 200-m ESTAR fields. We have already seen that the model variance, when aggregated to 200 m, is too large relative to the ESTAR data. If we perform the opposite comparison, using the value of the second moment of the ESTAR field at 200 m, 553, with $K(2) = -0.079$, we have the expected value of the second moment at 30 m as:

$$E[(\phi_\lambda)^2] \approx [30/200]^{-0.079} \times 553 = 642$$

For comparison, we convert this to the more familiar standard deviation in units of percent soil moisture by subtracting the square of the mean ESTAR soil moisture for that day (21.78%):

$$\sigma = [642 - [21.78]^2]^{1/2} = 12.9\%$$

The standard deviation of the model on that day at 30 m is about 14% (the standard deviation of the ESTAR imagery at 200 m is 6.6%, from Table 1). Note that in this calculation we have used the mean value of the ESTAR soil moisture field at 800 m, which is slightly different than the mean at 200 m, for reasons discussed below.

The above exercises illustrate the potential value of such a technique for scaling in terms of GIS-based modeling and remote sensing. In a given basin, it may be that log–log linearity of moment vs. scale for soil moisture holds under many different types of environmental conditions (as it did to some extent during the dry down at the Little Washita). Modeling or observation of soil moisture state over many scales would need to take place only to determine if this were true. Inferences about soil moisture variability could then be made by estimating the moments under the particular conditions from the most practical and available models and data. For example, for a very large basin, such as the Mississippi, limited studies across scales could be conducted to first determine scaling properties. The actual modeling could then take place using a model with coarse grid spacing from which $K(q)$ could be estimated at any particular time and inferences about variability at finer grid spacings made (however, see the section below on Caveats). Thus, even though $K(q)$ may change with environmental conditions, the scaling properties of the fields could be exploited to greatly reduce the required modeling.

In the best case, direct links may be made between the behavior of the $K(q)$ and environmental conditions such as vegetation, topography, and soils properties that affect the moisture fields. Such links may be central to understanding the physical mechanisms by which soil moisture variability is manifested across scales over the landscape. It might also limit the amount of small scale modeling and observation required by allowing prediction based on more easily attainable environmental data such as digital topography.

The preceding discussion and illustrations only are meant to show the potential applications within a multiscaling framework. Without a more solid physical basis from which the multiscaling properties of soil moisture fields are a natural theoretical consequence, such discussions must be considered premature, especially in an applied sense. However, exploratory analyses are valuable because they can provide evidence to support or refute a multiscaling hypothesis, and thus guide later investigations. Furthermore, from a pragmatic view, quantification of the spatial scaling properties of fields within a structured framework can aid our understanding of the most appropriate ways to integrate data from different scales within a modeling environment such as GIS.

Caveats

As cautioned earlier, exploration of multiscaling behavior, including the estimation of scaling exponents, is rarely an unambiguous process. First, the observation of log–log linearity over some range of scales is rather arbitrary. High correlation coefficients may be found for non-linear curves, as in Figure 4. Estimation over either the first half or second half of the second moment curves for the model fields would yield slightly different values of $K(q)$.

Secondly, each of the points in these curves is obtained from differing numbers of observations, and in general have different variances. Classically, when performing such a regression, weights for each point should be used inversely proportional to the variance. If the number of observations is great enough, for example if we have a large image, and do not aggregate over too many pixels, this should not be an issue; otherwise a weighted regression can always be performed.

The problem of missing data points is a concern as well. We did not use ESTAR aggregations that contained any missing data. Because even one 200-m missing data pixel could contaminate an entire 8×8 aggregation, the geographical support (area) over which the moments at the coarsest aggregation were calculated was different than that at full resolution. In other words, the effective support of the field is now no longer 2-D (two-dimensional), i.e., it is not completely plane filling, but rather will have some smaller dimensionality. Thus there is the dimensionality of the field itself (which is related to $K(q)$) as well as that of the underlying effective support. One way of seeing this is by comparing the means at each scale. For grid aggregations the means should all be equal. However, for the ESTAR data we observed that means decreased with scale on all days (for example on June 10 we observed a decrease from 22.57% to 21.3% as resolution decreased from fine to coarse). This decrease with scale also will be observed for the higher order moments. The dimensionality of the support area itself should then be considered as it may affect the estimation of $K(q)$. Note that the problem of the effective dimension of the support is caused here by the missing data and the procedure used to take these into account at coarser resolution. If all data were available, the effective dimension of the support would be equal to 2.

FURTHER REMARKS

We return to an aspect of scaling mentioned in the first section, that of non-linear transformations of input observations to output process fields. Although there is no room to discuss this at length here, a few points are worth considering given the general theme of this book. To reiterate, problems may occur because inputs are aggregated before transformation. For example, in performing our analyses of the ESTAR data we assume that the 200-m field is representative of soil moisture state, and analyze it by aggregating soil moisture values. We did not first aggregate the radiances, and then convert these radiances (non-linearly) to brightness temperatures (which is what takes place with a coarse resolution sensor). In the first case, we are examining the spatial scaling properties of the field at that resolution and beyond. In the latter we convolute the non-linearity of the transfer problem (Planck's equation) with that of the field itself at successive levels of aggregation (e.g., see Hall et al., 1992). We could always measure the soil moisture directly in the field without resorting to remote sensing, avoiding the Planck equation entirely, and find that the field is still multiscaling. This is because the Planck equation is not the generator of the spatial field (it is non-spatial), but merely a conversion from one type of observation to another. Multiscaling is concerned primarily with the scaling of the field itself, and not with such non-linear conversions, though the two may be linked

in ways that are not entirely clear yet (given that the radiances must be responsive to soil moisture state).

The same problem exists for modeled fields, i.e., aggregating input layers first and running a model vs. running a model and aggregating outputs. The focus typically is on whether or not model outputs scale linearly so that aggregated inputs may be used to model the process at large length scales. Generally, little emphasis is placed on understanding the spatial properties of the fields themselves. The reasons for this are not surprising. Given high computational (or observational costs) one would prefer to model on a coarse grid than a fine one, and utilize sub-grid scale parameterizations to correct for any important variability that may be missed. However, simply because similar means are obtained in aggregation experiments, this says little about the spatial scaling properties of the process, yet fields are routinely (and often incorrectly) labeled as "scaling" based on this criterion alone. The distinction here is between knowing whether a process (soil moisture, for example) is spatially scaling, as opposed to whether a particular *modeling procedure* leads to outputs whose means scale. These are not the same thing, though the latter is frequently taken for the former. There also has been little interest in predicting moments other than the mean, but recently it has been shown that for certain processes, including soil moisture, the second and higher order moments are of importance in a variety of applied ways (e.g., soil moisture variance may be related to the relative roles of atmospheric vs. land surface forcing). Furthermore, except for simple probability distributions, such as the normal distribution, all the statistical moments of order q are needed to have a complete description of the statistical properties of the fields. These issues are all complex and further research will be needed to resolve them.

SUMMARY

One of the fundamental issues of modeling is that of scale. The great potential of combining remotely sensed data within GIS-based modeling environments has yet to be realized. One reason for this is a lack of understanding about the nature of scaling problems. Most of the emphasis within both remote sensing and GIS has been placed on attempting to accurately reconstruct spatial means among scales in the presence of non-linear data and model transformations. These ad hoc attempts, while perhaps yielding problem-specific insights, have provided little guidance towards the creation of more generalized approaches. Such approaches may begin with a thorough treatment and statistical description of the spatial scaling properties of the geophysical fields themselves. This is because the spatial structures of fields routinely used in the earth sciences, whether surface temperature, vegetation indices, solar radiation or soil moisture, under differing environmental conditions, have not been adequately researched, nor have the physical mechanisms which give rise to this variability.

Multiscaling analysis may provide the basis for a more coherent exploration of scaling, particularly within the context of integrated modeling using remotely sensed data and GIS. Many geophysical fields are spatially heterogeneous, the result of

different spatially heterogeneous processes acting over different scales. Cascade processes can account for such heterogeneity while still producing variability which is organized (via multiscaling). Such fields are characterized by multiple scaling exponents that relate the moments of the field at one scale to those at another.

Both as an example of this approach, as well as an investigation of an important problem by itself, we have analyzed the multiscaling properties of remotely sensed and modeled soil moisture fields for a small basin. For both types of fields, we have found signals of multiscaling, namely, log–log linearity of statistical moment as a function of scale, and non-linear dependence of scaling exponents with order moment. This suggests that exploration of the physical mechanisms which lead to such behavior is appropriate. We have also shown how multiscaling, through the derivation of scaling exponents, may be used to infer spatial variability at scales other than the measurement scale. In particular, we demonstrated how a coarse remotely sensed field could be used to predict model variability at a much finer grid spacing. This ability may prove to be useful for the integration of remote sensing within GIS-based modeling.

One of the pioneers in remote sensing, David Simonett, frequently admonished his students to "pick a scale germane to the task." In the current era of global change research, this elementary truth has become increasingly difficult to put into practice. Multiscaling may be an important key, for it at least suggests the possibility of freeing the modeling process from the constraints imposed by the observational scale of inquiry.

ACKNOWLEDGMENTS

We thank Sara Loechel and Pete Peterson for useful inputs, and the anonymous reviewers for their thorough and helpful comments. This work was supported in part by NASA grant NAGW-2928, Department of Energy grant # DOE DE-FG03-90 ER61062, and the University of Maryland Institute for Advanced Computer Studies (UMIACS).

REFERENCES

Beven, K. and Kirkby, M., A physically based, variable contributing area model of basin hydrology, *Hydrol. Sci. Bull.*, 24, 43–69, 1979.

Davis, A., Marshak, A., and Wiscombe, W., Multifractal characterization of nonstationarity and intermittency in geophysical fields: Observed, retrieved or simulated, *J. Geophys. Res.*, 99, 8055–8072, 1994.

Dobson, M. C., Ulaby, F. T., Hallikainen, M. T., and Reyes, M., Microwave dielectric behavior of wet soils: II. Dielectric mixing models, *IEEE Trans. Geosci. Remote Sens.*, GE-23, 35–46, 1985.

Engman, E., Application of microwave remote sensing of soil moisture for water resources and agriculture, *Remote Sensing Environ.*, 35, 213–226, 1991.

Famiglietti, J. and Wood, E. F., Multiscale modeling of spatially variable water and energy balance processes, *Water Resour. Res.*, 30, 3061–3078, 1994a.

Famiglietti, J. and Wood, E. F., Application of multiscale water and energy balance models on a tallgrass prairie, *Water Resour. Res.*, 30, 3079–3093, 1994b.

Gupta, V. K. and Waymire, E. C., Multiscaling properties of spatial rainfall and river flow distributions, *J. Geophys. Res.*, 95, 1999–2009, 1990.

Gupta, V. K. and Waymire, E. C., A statistical analysis of mesoscale rainfall as a random cascade, *J. Appl. Meteorol.*, 32, 251–267, 1993.

Hall, F. G., Huemmrich, K. F., Goetz, S. J., Sellers, P. J., and Nickeson, J. E., Satellite remote sensing of surface energy balance: success, failures and unresolved issues in FIFE, *J. Geophys. Res.*, 97, 19061–19089, 1992.

Jackson, T. and LaVine, D. L., Mapping surface soil moisture using aircraft-based passive microwave radiometers, *NASA Soil Moisture Workshop: 25–27 Jan., 1994*, NASA, Tiburon, CA, 1994.

Jackson, T., LaVine, D. L., Griffis, A. J., Goodrich, D. C., Schmugge, T., Swift, C. T., and O'Neill, P., Soil moisture and rainfall estimation over a semi-arid environment with the ESTAR microwave radiomenter, *IEEE Trans. Geosci. Remote Sens.*, GE-31, 1993.

Jackson, T. and Schmugge, T., Passive microwave remote sensing of soil moisture, *Adv. Hydrosci.*, 14, 123–159, 1986.

Jackson, T. and Schmugge, T., Correction for the effects of vegetation on the microwave emission of soil, *IEEE IGARSS Digest*, 753–756, 1991.

Jourdan, D., Lavallée, D., Gautier, C., and Hooge, C., A study of the multifractal properties of the brightness temperatures of the TOPEX microwave radiometer, *Hydrofractals '93: Int. Conf. Fractals Hydrosci: 12–15 Oct., 1993, Lechia, Italy*, 1993.

Lavallée, D., Lovejoy, S., Schertzer, D., and Ladoy, P., Nonlinear variability, multifractal analysis and simulation of landscape topography, in *Fractals in Geography*, N. Lam and L. DeCola, Eds., Prentice Hall, Englewood Cliffs, NJ, 1993, 158–192.

Marshak, A., Davis, A., Cahalan, R., and Wiscombe, W. J., Bounded cascade models as nonstationary multifractals, *Phys. Rev. E*, 49, 55–69, 1994.

Meneveau, C. and Sreenivasan, K. R., Simple multifractal cascade model for fully developed turbulence, *Phys. Rev. Lett.*, 1424–1427, 1987.

Meneveau, C. and Sreenivasan, K. R., The multifractal nature of turbulent energy dissipation, *J. Fluid Mech.*, 224, 429–484, 1991.

Monin, A. S. and Yaglom, A. M., in *Statistical Fluid Mechanics*, Vol. 2, Cambridge University Press, London, 1987, 874.

Rawls, W. J., Brakensiek, D. L., and Saxton, K. E., Estimation of soil water properties, *Trans. ASAE*, 25, 1316–1320, 1982.

Rodriguez-Iturbe, I., Marani, M., Rigon, R., and Rinaldo, A., Self-organized river basin landscapes: fractal and multifractal characteristics, *Water Resour. Res.*, 30, 3531–3539, 1994.

Schertzer, D. and Lovejoy, S., Physically based rain and cloud modeling by anisotropic, multiplicative turbulent cascades, *J. Geophys. Res.*, 92, 9693–9714, 1987.

Schmitt, F., Lavallée, D., Schertzer, D., and Lovejoy, S., Empirical determination of universal multifractal exponents in turbulent velocity fields, *Phys. Rev. Lett.*, 68, 305–307, 1992.

Sellers, P., Heiser, M. D., Hall, F. G., Goetz, S. J., Strebel, P. E., Verma, S. B., Desjardins, R. L., Schuepp, P. M., and Mac Pherson, J. I., Effects of spatial variability in topography, vegetation cover and soil moisture on area-averaged surface fluxes: a case study using the FIFE 1989 data, *J. Geophys. Res.*, 100, 25,607–25,629, 1995.

Sellers, P. J., Hall, F. G., Asrar, G., Strebel, D. E., and Murphy, R. E., The first ISLSCP field experiment, *Bull. Am. Meteorol. Soc.*, 69, 22–27, 1988.

Tessier, Y., Lovejoy, S., and Schertzer, D., Universal multifractals: theory and observations for rain and clouds, *J. Appl. Meteor.*, 32, 223–250, 1993.

Wang, J. and Schmugge, T., An empirical model for the complex dielectric permittivity of soils as a function of water content, *IEEE Trans. Geosci. Remote Sens.*, GE-18, 288–295, 1980.

Weissel, J. K., Pratson, L. F., and Malinverno, A., The length-scaling properties of topography, *J. Geophys. Res.*, 99, 13997–14012, 1994.

Wood, E. F. and Lakshmi, V., Scaling water and energy fluxes in climate systems: three land-atmosphere modeling experiments, *J. Climate*, 6, 839–857, 1993.